

UCLA

UCLA Previously Published Works

Title

Analysis of transient Lamb waves generated by dynamic surface sources in thin composite plates

Permalink

<https://escholarship.org/uc/item/8qv1r2z3>

Journal

Journal of the Acoustical Society of America, 115(5)

ISSN

0001-4966

Authors

Banerjee, S
Mal, A K
Prosser, W H

Publication Date

2004-05-01

Peer reviewed

Analysis of transient Lamb waves generated by dynamic surface sources in thin composite plates

Sauvik Banerjee and Ajit K. Mal^{a)}

Mechanical and Aerospace Engineering Department, University of California, Los Angeles, California 90095-1597

William H. Prosser

Nondestructive Evaluation Branch, NASA Langley Research Center, MS 231, Hampton, Virginia 23681-0001

(Received 15 October 2003; revised 3 February 2004; accepted 10 February 2004)

A theoretical analysis is carried out in an effort to understand certain unusual properties of transient guided waves produced in a thin unidirectional graphite/epoxy composite plate by a localized dynamic surface load. The surface motion is calculated using an approximate plate theory, called the shear deformation plate theory (SDPT), as well as a recently developed finite element analysis (FEA), for their mutual verification. The results obtained by the two methods are shown to have excellent agreement. An interesting, nearly periodic “phase reversal” of the signal with propagation distance is observed for each propagation direction relative to the fiber direction. For clarification, a closed form analytical expression for the vertical surface displacement in an aluminum plate to an impulsive point force is obtained using the steepest descent method. It is found that the strong dispersion of the first antisymmetric waves at low frequencies is the main reason behind the phase reversal. This is verified further by measuring the surface response of a relatively thick aluminum plate to a pencil lead break source. The understanding developed in the paper is expected to be helpful in detecting and characterizing the occurrence of damage in composite structures. © 2004 Acoustical Society of America. [DOI: 10.1121/1.1694993]

PACS numbers: 43.20.Bi, 43.35.Cg, 43.40.Le [ANN]

Pages: 1905–1911

I. INTRODUCTION

Advanced composites are being used increasingly in aircraft, aerospace, marine, automotive and other structures, due to their high strength to weight ratio, formability and other favorable properties. However, these materials are highly sensitive to the presence of manufacturing and service related defects. As an example, graphite/epoxy laminate, one of the most widely used composite structural components, can sustain hidden internal damage (delamination, fiber breakage, matrix cracking) when it is subjected to foreign object impact. If undetected, the damage can grow, leading to catastrophic failure of the structure. Detection and characterization of hidden flaws in composites are critical factors for continued safe operation of advanced defects critical structures.

Ultrasonic nondestructive evaluation (NDE) techniques offer an efficient and accurate procedure for damage monitoring in composite structures. In order to develop reliable damage monitoring systems, it is necessary to have a clear understanding of the quantitative nature of ultrasonic waves that can be transmitted in composite laminates.

Propagation of elastic waves in isotropic solids has been investigated in great detail for several decades due to its importance in seismology¹ and ultrasonic nondestructive evaluation.² Waves in beams and plates have also been the subject of a large number of studies³ since they are widely used in a variety of engineered structures. In contrast, wave

propagation studies in structural composites are of relatively recent origin.^{4,5} Since the composite laminates used in aircraft and aerospace structures are usually thin, approximate thin-plate theories have been developed in an effort to gain model-based understanding of the nature of the guided waves that can be transmitted in them.

The more important and relevant class of problems where the waves are generated by surface or subsurface sources is less well studied and is a topic of considerable current research interest. The solution of three-dimensional problems consisting of multilayered, angle-ply laminates of finite thickness and large lateral dimensions subjected to various types of surface loads has been given in Refs. 6–8. The finite element method (FEM) has also been used as an alternative to solve these problems. A dynamic finite element code has been developed by NIST for the prediction of AE wave propagation in plates.⁹ This code has been validated with both experimental measurements and analytical predictions for a variety of source conditions and plate dimensions in isotropic materials.^{9–11} However, these so-called “exact” methods are computationally intensive and cannot generally be used in damage monitoring systems, where data collected by on-board sensors must be analyzed in real-time.

As indicated earlier, in thin-walled aircraft and aerospace structures, approximate solutions based on thin plate theories can provide reasonably accurate numerical results with negligible computational effort. It has been shown that the approximate SDPT, where the transverse shear and rotary inertia are retained in modeling the dynamic deformations across the thickness of the plate, can provide accurate waveforms at lower frequencies (i.e., the plate thickness is small

^{a)} Author to whom correspondence should be addressed. Electronic mail: ajit@ucla.edu

compared to the wavelength) and at some distance away from the source.¹² In this paper, the approximate method is used to calculate the response of a thin unidirectional composite plate to a concentrated force on the surface of the plate. The results from SDPT are compared with those from FEM for their mutual verification. A previously unknown feature of the surface motion, namely, a complete and spatially periodic reversal of the initial phase of the displacement pulse, is observed in the calculated waveforms using both methods. Since these methods are primarily numerical in nature, they do not provide a clear explanation of the reason behind this behavior of the waveforms. An approximate closed form analytical expression for the far field displacement produced by a surface line load on an isotropic plate is derived and is shown to have the same general feature. The analytical solution shows that the phase reversal is caused by the strong dispersion of the guided first antisymmetric or flexural waves in the plate.

II. NUMERICAL SOLUTIONS

The first order SDPT retaining transverse shear and rotary inertia of the plate elements is used here. Assuming that the x - y plane is the mid-plane of the laminate, the displacement components within the laminate are assumed to be of the form

$$u(x, y, z, t) = u_0(x, y, t) + z\psi_x(x, y, t),$$

$$v(x, y, z, t) = v_0(x, y, t) + z\psi_y(x, y, t),$$

$$w(x, y, z, t) = w_0(x, y, t),$$

where (u_0, v_0, w_0) are the displacement components at a point in the mid-plane, and ψ_x and ψ_y are the rotations of a line element, originally perpendicular to the longitudinal plane, about the y and x axes, respectively. The solution of the resulting approximate system of equations can be obtained using multiple integral transforms. A detailed formulation on first order SDPT for wave field calculations in composite laminates can be found in Ref. 12 and the associated literature cited therein, and will not be repeated here. In general, the Fourier time transform of the displacement and stress components on the surface of the laminate can be expressed as wavenumber integrals in the form

$$F(\omega) \int_{-\infty}^{\infty} \int_{-\infty}^{\infty} g(k_1, k_2, \omega) e^{i(k_1 x_1 + k_2 x_2)} dk_1 dk_2,$$

where ω is the circular frequency, $F(\omega)$ is the Fourier time transform of the source function, $f(t)$, x_1, x_2 are the coordinates of the field point on the surface of the plate with the x_1 -axis directed along the fibers, and the function g is determined from the equations of motion and the boundary conditions of the problem. These integrals must, in general, be evaluated numerically for a range of frequencies and the resulting spectra can then be inverted by FFT to determine the time dependent displacement and stress components. The computational effort required to evaluate the integrals numerically accurately is quite large. An adaptive integration scheme developed in Ref. 12 is used to calculate the surface motion. It should be noted that the result includes both the body and guided wave contributions, however, at lower fre-

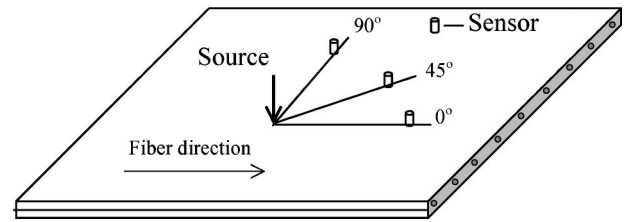


FIG. 1. Schematic of a loaded unidirectional composite plate showing position of the sensors wrt the fiber direction.

quencies most of the energy in the plate is carried by the first antisymmetric guided wave or the A_0 mode.

The normal surface displacement in a unidirectional graphite/epoxy composite plate to a normal point load on the surface calculated from the SDPT and FEM is presented first. A loaded unidirectional composite plate with surface mounted sensors is shown in Fig. 1. The elastic properties of the graphite/epoxy composite material used in the calculations are given in Table I.

The plate thickness is taken as 1 mm and the load is assumed to be of the form

$$F(x_1, x_2, t) = f(t)g(x_1, x_2), \quad (1)$$

where

$$f(t) = \sin\left(\frac{2\pi t}{\tau}\right) - 0.5 \sin\left(\frac{4\pi t}{\tau}\right), \quad 0 < t < \tau, \\ = 0, \quad t > \tau. \quad (2)$$

For a point load,

$$g(x_1, x_2) = \delta(x_1)\delta(x_2), \quad (3a)$$

and for a load uniformly distributed in a circle of radius a ,

$$g(x_1, x_2) = 1, \quad x_1^2 + x_2^2 \leq a^2 \\ = 0, \quad x_1^2 + x_2^2 \geq a^2. \quad (3b)$$

The time dependence of the load $f(t)$ and its Fourier transform are plotted for $\tau = 1 \mu s$ in Fig. 2. It can be seen that the source spectrum is maximum around 1.1 MHz and becomes negligibly small beyond 3 MHz.

The results obtained from the SDPT for the vertical surface displacement at a number of field points are compared with those from FEM in Figs. 3(a)–(c) for propagation along 0° , 45° , and 90° with respect to the fiber direction. A third-order elliptic digital filter (Matlab 6.1) with a pass band of 0.05–0.65 MHz is applied to all calculated spectra to eliminate high frequency numerical noise. It can be seen that the agreement between the results from the two methods is excellent. Since the approximate theory (SDPT) overestimates the flexural wave speed,¹² the arrival time of waves in this case is somewhat earlier than that in the FEM.

TABLE I. Material constants of graphite/epoxy composite material.

Density (g/cm ³)	C ₁₁ (GPa)	C ₁₂ (GPa)	C ₂₂ (GPa)	C ₂₃ (GPa)	C ₅₅ (GPa)
1.578	160.73	6.44	13.92	6.92	7.07

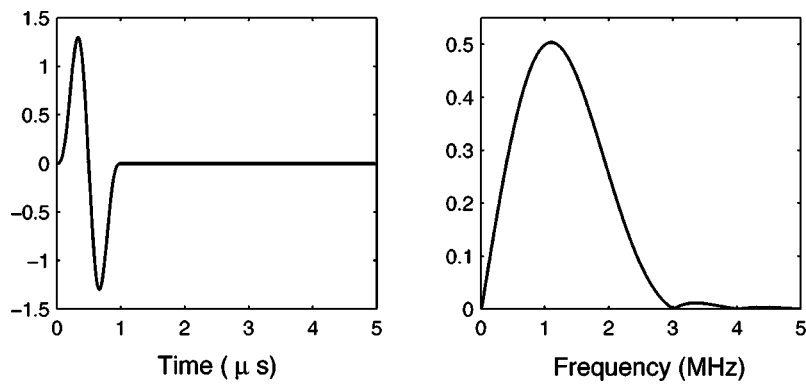


FIG. 2. Time history and spectrum of the source in arbitrary units.

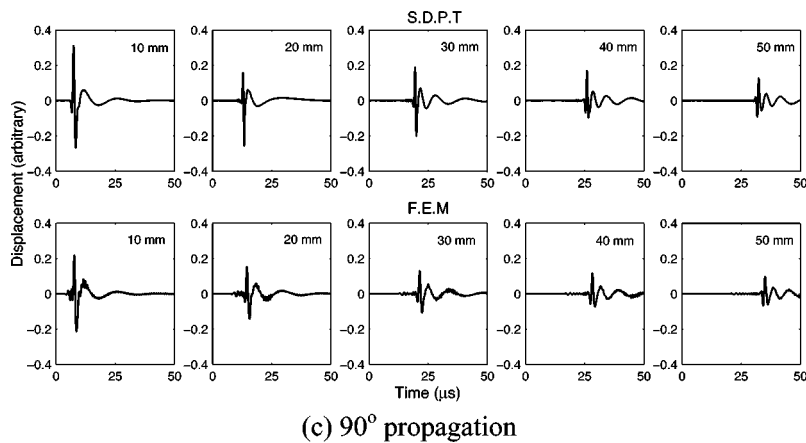
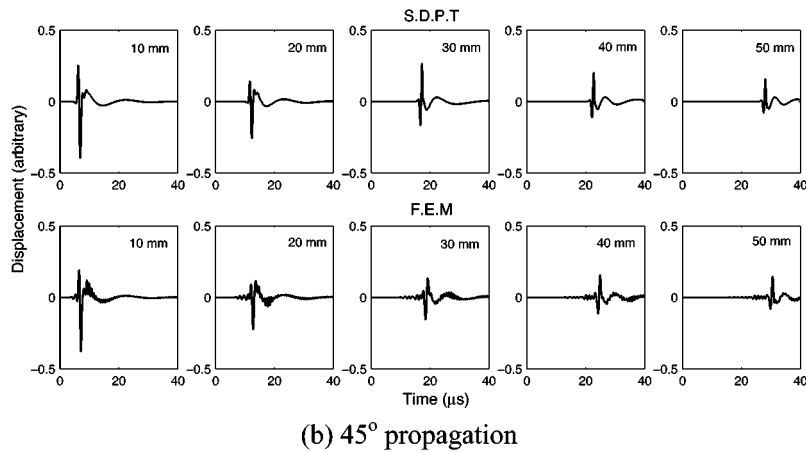
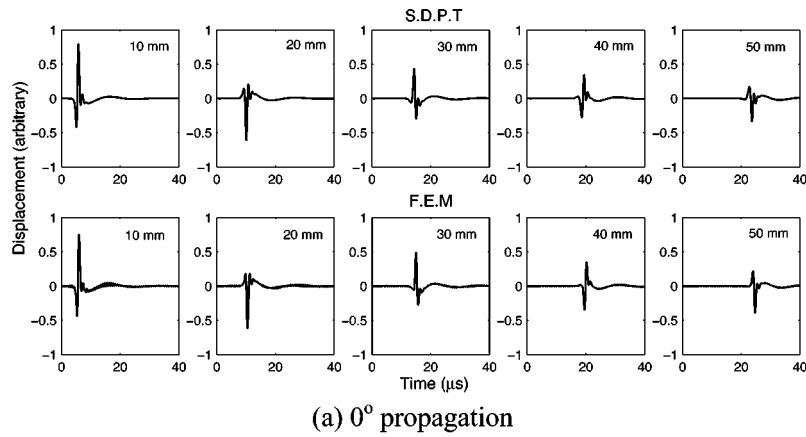


FIG. 3. Time history of vertical surface displacement in a 1-mm-thick unidirectional graphite/epoxy composite plate subjected to a point load from SDPT (first row) and FEM (second row).

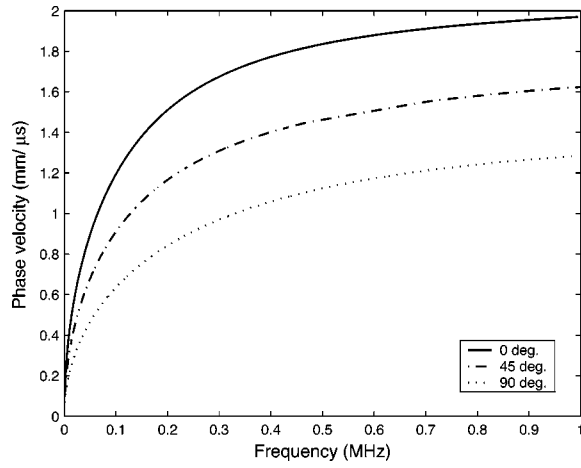


FIG. 4. Dispersion curves for unidirectional graphite/epoxy composite plate of 1-mm thickness for different propagation direction wrt the fibers calculated from SDPT.

The most noteworthy feature of the surface displacements calculated by both methods is a periodic reversal in the initial phase of the pulse with propagation distance. For propagation along 0° [Fig. 3(a)], the reversal occurs at an interval of 10 mm, whereas it occurs at larger intervals for propagation along 45° [Fig. 3(b)]; the interval is the largest for propagation along 90° [Fig. 3(c)]. This is due to faster flexural wave speed along 0° direction as shown in the dis-

persion curves for the plate for different propagation directions (Fig. 4). Figure 5 shows the response at distances between 10 and 20 mm at an interval of 2 mm for propagation along 0° . It can be seen that the rising first peak and decaying second peak result in a smooth reversal of phase at an interval of 10 mm.

The time history of the surface displacement due to a uniform distributed surface load on a 2.5-mm-radius circular region is shown in Fig. 6 for propagation along 0° at different locations. The periodic reversal in the phase is found in this case, too. The waveforms do not change as significantly as in the point load case, and their sharpness is reduced considerably due to the spatial distribution of the load.

III. PHASE REVERSAL: THEORETICAL AND EXPERIMENTAL VALIDATION

The phase reversal of the surface displacement is difficult to explain from the primarily numerical methods used in both the SDPT and the FEM. A simpler problem for which an analytical solution can be obtained is considered here in an effort to understand the source of this behavior of the guided waves. The problem involves an isotropic (aluminum) plate of thickness $2H$ subjected to a normal concentrated line load. Considering only A0 mode, the Fourier transform of the normal surface displacement, V , can be expressed in the form

$$V(x, H, \omega) = \frac{F(\omega)}{4\pi\mu} \int_{-\infty}^{\infty} \frac{k_2^2 \eta_1 e^{ikx}}{(2k^2 - k_2^2)^2 \tanh(\eta_1 H) - 4k^2 \eta_1 \eta_2 \tanh(\eta_2 H)} dk, \quad (4)$$

where

$$\eta_j = \sqrt{k^2 - k_j^2}; \quad k_j = \frac{\omega}{c_j}, \quad j = 1, 2,$$

c_1 and c_2 are the longitudinal and shear wave speeds in the material of the plate, $F(\omega)$ is the Fourier time transform of the load and μ is the shear modulus.

At low frequencies, when the plate thickness is small compared to the wavelength, the quantities kH , k_1H , k_2H

are small. Then, retaining the first two terms in the Taylor series expansion of $\tanh(\eta_1 H)$ and $\tanh(\eta_2 H)$, Eq. (4) can be rewritten as

$$V(x, H, \omega) = \frac{F(\omega)}{4\pi\mu} \int_{-\infty}^{\infty} \frac{(k_2^2/H) e^{ikx}}{R(k)} dk, \quad (5)$$

where

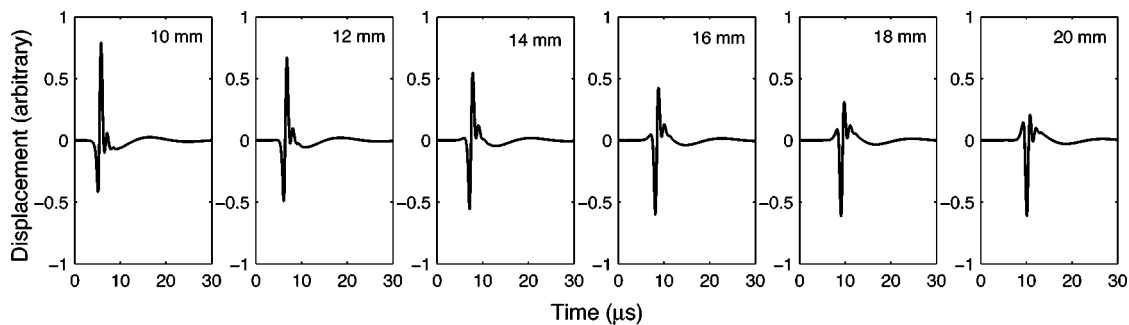


FIG. 5. Time history of vertical surface displacement in a 1-mm-thick unidirectional graphite/epoxy composite plate subjected to a point load at an interval of 2 mm in between 10 and 20 mm, showing smooth change in phase, for 0° propagation (SDPT).

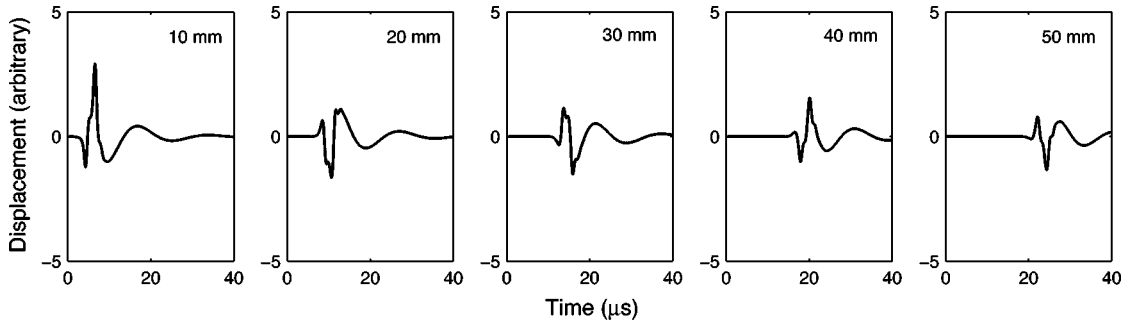


FIG. 6. Time history of vertical surface displacement in a 1-mm-thick unidirectional graphite/epoxy composite plate under uniformly distributed load on a circle of 2.5-mm radius, for propagation along 0° (SDPT).

$$R(k) = k_2^4 - \frac{4}{3}k^4(k_2H)^2(1 - \alpha^2) - k^2 \frac{(k_2H)^2}{3} \times k_2^2(4\alpha^2 - 3) + k_2^4 \frac{(k_1H)^2}{3} + O[(k_1H)^3], \quad (6)$$

and $\alpha = k_1/k_2 = c_2/c_1$. The last term in (6) is third order in k_1H and is neglected in further calculations.

Applying the contour integration technique in the complex k -plane, the propagating guided wave contribution to the surface displacement is given by the residue at the pole of the integrand as

$$V(x, H, \omega) \cong \frac{iF(\omega)}{2\mu} \frac{(k_2^2/H)e^{ik_p x}}{R'(k_p)} \quad (7)$$

where k_p , the wavenumber of the guided waves in the plate, is a real root of $R(k) = 0$. Assuming that the material of the plate is aluminum, $\alpha = \frac{1}{2}$,

$$R(k) \cong -\frac{k_2^2}{H^2} \left\{ (kH)^4 - \frac{2}{3}(kH)^2(k_2H)^2 - (k_2H)^2 \times \left(1 + \frac{(k_2H)^2}{12} \right) \right\} \quad (8)$$

and

$$R'(k) \cong -\frac{4k_2^2}{H} (kH) \left[(kH)^2 - \frac{1}{3}(k_2H)^2 \right]. \quad (9)$$

Then the root of $R(k)$ is given by the approximate expression

$$k_p H \cong \sqrt{k_2 H} \left[1 + \frac{1}{6}(k_2 H) \right] \quad (10)$$

or

$$k_2 H \cong (k_p H)^2 \left[1 - \frac{1}{3}(k_p H)^2 \right]. \quad (11)$$

The time dependent displacement can be written in the alternate integral form as

$$v(x, H, t) = \frac{1}{2\pi} \int_{-\infty}^{\infty} V(x, H, \omega) e^{-i\omega t} d\omega = \int_{-\infty}^{\infty} G(k) e^{i[kx - \omega(k)t]} dk, \quad (12)$$

where

$$G(k) = \frac{1}{2\pi} V(x, H, \omega) \frac{d\omega}{dk}. \quad (13)$$

In general, the integral in (12) must be evaluated numerically to obtain the pulse shape of the traveling waves. We use the steepest descent method to derive an approximate analytical expression for the integral. The stationary values of the exponent $g(k) = kx - \omega(k)t$ occurs near the values of k given by

$$\frac{d\omega}{dk} = \frac{x}{t} = U(k), \quad (14)$$

where $U(k)$ is the group velocity of the plate guided waves. From Eq. (11),

$$\frac{\omega H}{c_2} = (kH)^2 - \frac{1}{3}(kH)^4 \quad (15)$$

so that

$$\frac{d\omega}{dk} = 2c_2 k H \left[1 - \frac{2}{3}(kH)^2 \right] = \frac{x}{t}. \quad (16)$$

Let the solution of (14) and (16) be $k = k_o$ and $\omega_o = \omega(k_o)$. Then

$$k_o H \cong \frac{x}{2c_2 t} + \frac{2}{3} \left(\frac{x}{2c_2 t} \right)^3 \quad (17)$$

and

$$\omega_o \cong \frac{c_2}{H} \left[\left(\frac{x}{2c_2 t} \right)^2 + \left(\frac{x}{2c_2 t} \right)^4 \right]. \quad (18)$$

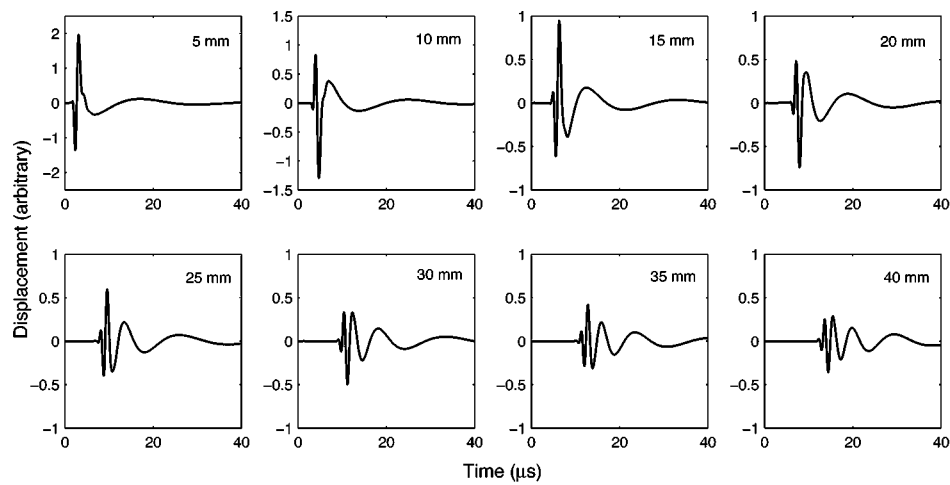
Therefore,

$$k_o x - \omega_o t \cong \frac{x^2}{4c_2 t H} + \frac{x^4}{48(c_2 t)^3 H}. \quad (19)$$

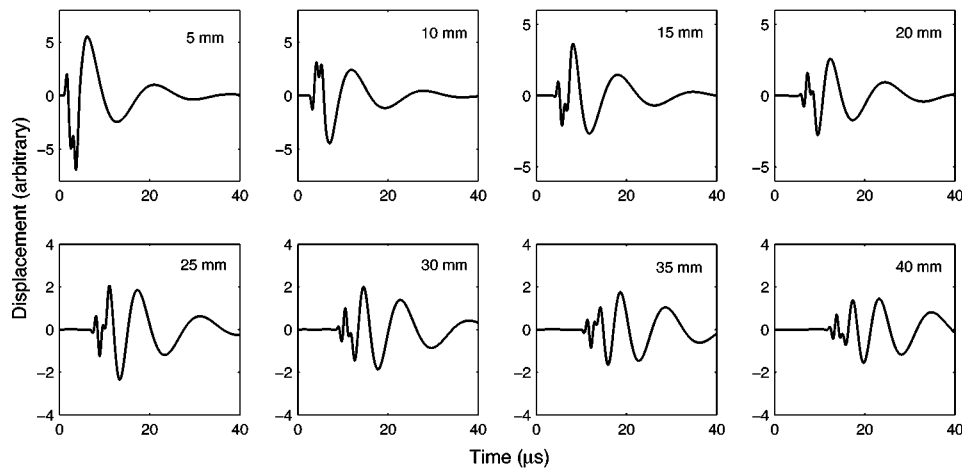
Expanding $g(k)$ in a Taylor series about $k = k_o$ and, after some manipulation, the integral (12) gives

$$v(x, H, t) = \left\{ \left[\frac{2\pi}{|-g''(k_o)|} \right]^{1/2} G(k_o) e^{i[g(k_o) - \pi/4]} \right\}. \quad (20)$$

Retaining second order terms in the nondimensional quantity, $x/2c_2 t$, the analytical expression for the normalized surface displacement, \bar{v} , due to a source of time dependence $f(t) = S_o \delta(t)$ in an aluminum plate can be written explicitly as



(a)



(b)

FIG. 7. Time history of vertical surface displacement in a 1-mm-thick aluminum plate subjected to (a) a point load and (b) a uniformly distributed load on a 2.5-mm radius (SDPT).

$$\bar{v} = \frac{v(x, H, t)}{S_o c_2 / 8 \pi \mu H}$$

$$\cong \sqrt{\frac{\pi H}{c_2 t}} \frac{1 - \frac{2}{3} (x/2c_2 t)^2}{(x/2c_2 t)^2 \sqrt{1 - 2(x/2c_2 t)^2}} \sin \left[\frac{x^2}{4c_2 H t} - \frac{\pi}{4} \right]. \quad (21)$$

It can be seen that expression (21) carries a singularity that travels with a speed $V_s = \sqrt{2}c_2$, and that

$$\bar{v} > 0, \text{ for } 2\sqrt{2} \left(2n + \frac{1}{4} \right) \pi < \frac{x}{H} < 2\sqrt{2} \left(2n + \frac{5}{4} \right) \pi,$$

$$\bar{v} < 0, \text{ for } 2\sqrt{2} \left(2n + \frac{5}{4} \right) \pi < \frac{x}{H} < 2\sqrt{2} \left(2n + \frac{9}{4} \right) \pi,$$

where n is a positive integer. Thus the distance required for a complete phase reversal of this singularity in the waveform is given by $2\sqrt{2}\pi H$.

The response of the aluminum plate to the normal surface load is calculated using SDPT. The vertical surface displacement produced in an aluminum plate of 1-mm thickness by the point and distributed loads used earlier in the composite plate case are plotted in Fig. 7 at an interval of 5 mm up

to 40 mm. The same band pass filter as that of composite plate case is applied to the spectra before inversion into time domain. The numerical results show that the surface response reverses its phase at an interval of approximately 5 mm, or $2\sqrt{2}\pi H$ as predicted by the approximate analytical solution. However, this effect becomes negligible at large distances from the source.

The calculated and measured signals for the Hsu–Neilsen-type pencil lead break source^{13,14} are also shown in Fig. 8 for an aluminum plate of thickness 3.1. The detail of the experimental setup¹⁴ is omitted here for brevity. Both calculated and experimentally acquired waveforms are normalized relative to their individual peak amplitudes. The resulting acoustic emission plots show good agreement for every separation distance between the lead break location and the recording transducer. Note that after the first few wiggles in acoustic emission time-history, reflections are seen in experimentally acquired waveforms. Since the experimentally acquired waveform is triggered by a constant triggering transducer at a fixed distance away from the source and is not plotted on an absolute time scale, only the waveforms and the relative times between the two plots can be compared. More notably, phase reversal is seen at an interval of

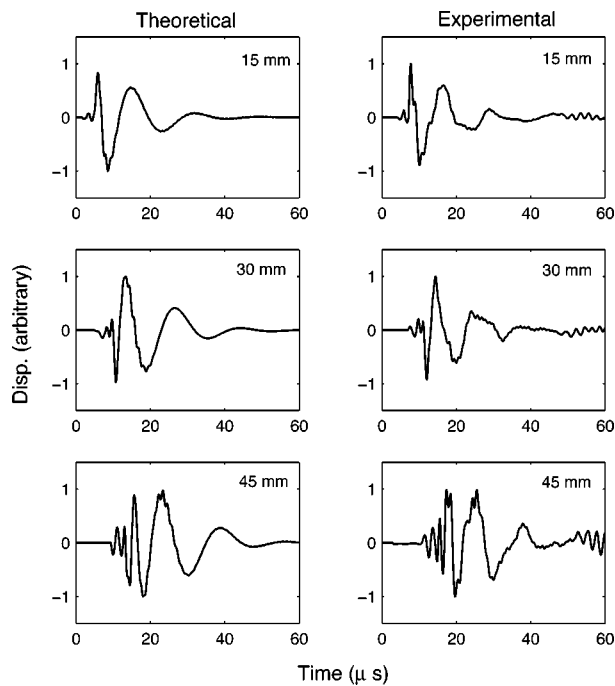


FIG. 8. Time history of vertical surface displacement in a 3.1-mm-thick aluminum plate to a pencil lead break source.

approximately $15 \text{ mm} (\approx 2\sqrt{2}\pi H)$, which was deliberately chosen as a recording interval for the test.

IV. CONCLUDING REMARKS

The good agreement between the results from SDPT and FEM indicates that both methods work well for the calculation of the wave field produced in a plate by localized dynamic sources. Since the SDPT is expected to be more accurate at larger distances from the source, while the FEM is more efficient at smaller distances, the two methods can be combined for efficient and accurate calculation of the waveforms in plates. This capability is expected to be helpful in the accurate characterization of AE sources, and to enhance the accuracy of data interpretation for online monitoring of impact damage critical structural components.

Although the closed form analytical expression (21) differs significantly from the exact solution, the usefulness of

the approximate solution to understand the physics of the problem cannot be overemphasized. The approximate solution clearly shows that the dispersive nature of waves is the source of the unexpected phase reversal of the waveforms during propagation on the surface of the plate. It should be recalled that the low frequency symmetric or extensional waves do not have this property, nor do nondispersive Rayleigh waves propagating in a half-space.

ACKNOWLEDGMENT

This research was supported by NASA Langley Research Center under Grant No. NAG-1-02036.

- ¹K. Aki and P. G. Richards, *Quantitative Seismology: Theory and Methods* (Freeman, San Francisco, 1980).
- ²J. D. Achenbach, *Wave Propagation in Elastic Solids* (North-Holland, Amsterdam, 1973).
- ³J. L. Rose, *Ultrasonic Waves in Solid Media* (Cambridge U.P., New York, 1999).
- ⁴A. H. Nayfeh, *Wave Propagation in Layered Anisotropic Media with Applications to Composites* (Elsevier, Amsterdam, 1995).
- ⁵D. E. Chimenti, "Guided waves in plates and their use in material characterization," *Appl. Mech. Rev.* **50**, 247–284 (1997).
- ⁶A. K. Mal, "Wave propagation in layered composite laminates under periodic surface loads," *Wave Motion* **10**, 257–266 (1988).
- ⁷A. K. Mal and S. S. Lih, "Elastodynamic response of a unidirectional composite laminate to concentrated surface loads: parts I & II," *J. Appl. Mech.* **55**, 878–892 (1992).
- ⁸S. S. Lih and A. K. Mal, "Response of multilayered composite laminates to dynamic surface loads," *Composites, Part B* **27B**, 633–641 (1996).
- ⁹W. H. Prosser, M. A. Hamstad, J. Gary, and A. O'Gallagher, "Comparison of finite element and plate theory methods for modeling acoustic emission waveforms," *J. Nondestruct. Eval.* **18**(3), 83–90 (1999).
- ¹⁰J. Gary and M. A. Hamstad, "On the far-field structure of waves generated by a pencil break on a thin plate," *J. Acoust. Emiss.* **12**(3-4), 157–170 (1994).
- ¹¹D. Guo, A. K. Mal, and M. A. Hamstad, "AE wavefield calculations in a plate," *J. Acoust. Emiss.* **16**(1-4), S222–S232 (1998).
- ¹²S. S. Lih and A. K. Mal, "On the accuracy of approximate plate theories for wave field calculations in composite laminates," *Wave Motion* **21**, 17–34 (1995).
- ¹³F. Breckenridge, T. Proctor, N. Hsu, S. Fick, and D. Eitzen, "Transient sources for acoustic emission work," in *Progress in Acoustic Emission V*, edited by K. Yamguchi, H. Takakashi, and H. Niitsuma (JSNDI, Tokyo, Japan, 1990), pp. 20–37.
- ¹⁴D. Guo, A. K. Mal, and K. Ono, "Wave theory of acoustic emission in composite laminates," *J. Acoust. Emiss.* **14**, S19–S46 (1996).